

Comparative study of air gap, direct contact and sweeping gas membrane distillation configurations

Nizar Loussif^{*1,2} and Jamel Orfi³

¹ Ecole Nationale d'Ingénieur de Monastir, Université de Monastir, Monastir, Tunisia

² Unité de Recherche Matériaux, Energie et Energies Renouvelables,
Faculté des Sciences Gafsa, Université de Gafsa, 2100 Gafsa, Tunisia

³ Department of Mechanical Engineering, College of Engineering, King Saud University, Riyadh, Saudi Arabia

(Received September 01, 2015, Revised December 08, 2015, Accepted December 18, 2015)

Abstract. The present study deals with a numerical simulation for the transport phenomena in three configurations of Membrane Distillation (Air Gap, Direct Contact and Sweeping Gas Membrane Distillation) usually used for desalination in order to make an objective comparison between them under the same operating conditions. The models are based on the conservation equations for the mass, momentum, energy and species within the feed saline and cooling solutions as well as on the mass and energy balances on the membrane sides. The theoretical model was validated with available data and was found in good agreement. DCMD configuration provided the highest pure water production while SGMD shows the highest thermal efficiency. Process parameters' impact on each configuration are also presented and discussed.

Keywords: desalination; membrane distillation; air gap; direct contact; sweeping gas

1. Introduction

Nowadays, many techniques are used to produce pure water. As a promising technique, membrane distillation (MD); has many advantages particularly low energy consumption. In Membrane distillation, a hydrophobic membrane is used to avoid membrane wetting and permitting only vapor transport; the driving force is the difference in vapor pressure of water caused by a temperature difference across the membrane. In fact, vapor molecules are transported from the high vapor pressure side to the low vapor pressure side. This vapor pressure difference may be maintained with one of the four following possibilities applied on the permeate side which leads to four different configurations (Rommel *et al.* 2007, El-Bourawi *et al.* 2006):

- An aqueous solution colder than the feed solution maintained in the direct contact with the permeate side; this configuration is known as Direct Contact Membrane Distillation (DCMD).
- A cold gas sweeps the permeate side carrying the water vapor molecules outside the membrane module where the condensation takes place; this configuration is termed Sweeping Gas Membrane Distillation (SGMD).

*Corresponding author, Nizar Loussif, Ph.D., E-mail: loussif_nizare@yahoo.fr

- An air gap is placed between the membrane and a condensation surface; the water vapor molecules cross the membrane and the stagnant air and condense on the internal side of a cooling plate; this configuration is known as Air Gap Membrane Distillation (AGMD).
- A vacuum pump can be used to reduce the pressure in the permeate side; the condensation occurs outside of the membrane module; this configuration is termed Vacuum Membrane Distillation (VMD).

Many experimental and theoretical investigations have been done to show MD performance expressed in particular the pure water production and the thermal efficiency.

One can observe that many experimental studies have been done covering all configurations particularly AGMD (Feng *et al.* 2008, García-Payo *et al.* 2000, Guijt *et al.* 1999, 2005, Izquierdo-Gil *et al.* 1999, Amali *et al.* 2004, Sebastian *et al.* 2006), DCMD (Gryta *et al.* 2006, Srisurichan *et al.* 2006, Tomaszewska *et al.* 1995, Christensen *et al.* 2006, Song *et al.* 2008, Chang *et al.* 2014), VMD (Gábor *et al.* 2015, Chen *et al.* 2015, Wu *et al.* 2015) and SGMD (García-Payo *et al.* 2002, Khayet *et al.* 2000a, 2003a, Charfi *et al.* 2010, Shirazi *et al.* 2014).

Furthermore, the theoretical studies concerned with the membrane distillation (MD) process are conducted with many assumptions describing for example the flow regime and the heat and mass transfer process: AGMD (Banat and Simandl 1994, Alklaibi and Lior 2005, Banat and Simandl 1998, Loussif and Orfi 2014), DCMD (Banat and Simandl 1998, Schofield and Fane 1987, Phattaranawik *et al.* 2003), SGMD (Khayet *et al.* 2000b, Charfi *et al.* 2010, Khayet *et al.* 2002). Now, one can have a reasonable question, which configuration is the best in term of energy requirement and pure water production?

It is worth to mention that just few studies were conducted with the main objective to compare the performance of the MD configurations. Among these studies, Ding *et al.* 2006 and Khayet *et al.* 2003a have performed experimental works for ammonia removal from water and nuclear desalination applications respectively.

The purpose of this study is to present a theoretical, two-dimensional model of the transport phenomena in AGMD, DCMD and SGMD modules and to conduct a comparative analysis under the same operating conditions.

2. Mathematical model

2.1 Process description

In this study, we will focus on the comparison of three configurations used in MD: Air-Gap Membrane Distillation (AGMD), Direct Contact Membrane Distillation (DCMD) in which pure water is used as a coolant flow and the Sweeping Gas Membrane Distillation (SGMD). Fig. 1(a) represents a schematic of air-gap membrane distillation (AGMD). The removal of the cooling plate, the condensate film and the air –gap gives the direct contact membrane distillation (DCMD). In the obtained DCMD process, replacing cold water flow by an air flow leads to the SGMD process together presented in Fig. 1(b).

2.2 Governing equations

In this section, we will present the governing equations and their boundary conditions for the AGMD process, and as mentioned in the previous section, we simplify the model to obtain the DCMD and SGMD processes.

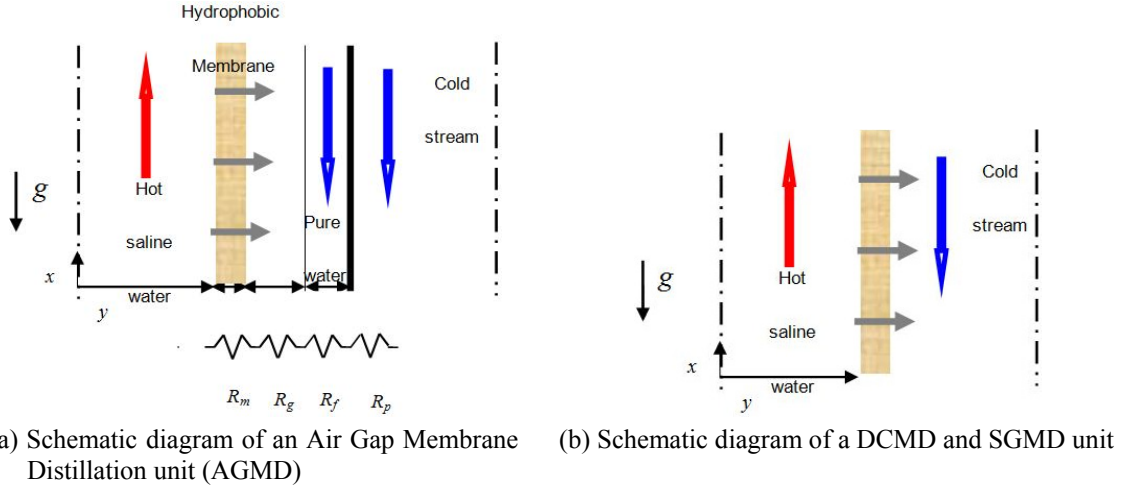


Fig. 1 Geometry and coordinate system of flow domain

The partial differential equations governing the flow, heat and mass transfer within the hot feed saline water and the coolant solution (pure water) are those of conservation of mass, momentum energy and species in x and y directions.

These equations can be normalized using the following dimensionless variables (the suffixes 1 and 2 represent respectively the hot saline solution and the cold pure water).

$$\bar{x} = \frac{x}{l_1}, \quad \bar{y} = \frac{y}{l_1}, \quad \bar{U} = \frac{U}{U_{in1}}, \quad \bar{V} = \frac{V}{U_{in1}}, \quad \bar{P} = \frac{P}{\rho_1 U_{in1}^2}, \quad \bar{T} = \frac{T - T_{in2}}{T_{in1} - T_{in2}}, \quad \bar{C} = \frac{C}{C_{in1}} \quad (1)$$

$$\bar{x} = \frac{x}{l_2}, \quad \bar{y} = \frac{y}{l_2}, \quad \bar{U} = \frac{U}{U_{in2}}, \quad \bar{V} = \frac{V}{U_{in2}}, \quad \bar{P} = \frac{P}{\rho_2 U_{in2}^2}, \quad \bar{T} = \frac{T - T_{in2}}{T_{in1} - T_{in2}} \quad (2)$$

So we obtain in the hot domain

$$\frac{\partial \bar{U}}{\partial x} + \frac{\partial \bar{V}}{\partial x} = 0 \quad (3)$$

$$\bar{U} \frac{\partial \bar{U}}{\partial x} + \bar{V} \frac{\partial \bar{U}}{\partial y} = -\frac{\partial \bar{P}}{\partial x} + \frac{1}{\text{Re}_1} \left(\frac{\partial^2 \bar{U}}{\partial x^2} + \frac{\partial^2 \bar{U}}{\partial y^2} \right) \quad (4)$$

$$\bar{U} \frac{\partial \bar{V}}{\partial x} + \bar{V} \frac{\partial \bar{V}}{\partial y} = -\frac{\partial \bar{P}}{\partial x} + \frac{1}{\text{Re}_1} \left(\frac{\partial^2 \bar{V}}{\partial x^2} + \frac{\partial^2 \bar{V}}{\partial y^2} \right) \quad (5)$$

$$\bar{U} \frac{\partial \bar{T}}{\partial x} + \bar{V} \frac{\partial \bar{T}}{\partial y} = \frac{1}{\text{Re}_1 \text{Pr}_1} \left(\frac{\partial^2 \bar{T}}{\partial x^2} + \frac{\partial^2 \bar{T}}{\partial y^2} \right) \quad (6)$$

$$\bar{U} \frac{\partial \bar{C}}{\partial x} + \bar{V} \frac{\partial \bar{C}}{\partial y} = \frac{1}{\text{Re}_1 \text{Sc}_1} \left(\frac{\partial^2 \bar{C}}{\partial x^2} + \frac{\partial^2 \bar{C}}{\partial y^2} \right) \quad (7)$$

Where the Reynolds, Prandlt and Schmidt of the hot saline solution are

$$\text{Re}_1 = \frac{\rho_1 U_{in1} l_1}{\mu_1}, \quad \text{Pr}_1 = \frac{\mu_1 C_{p1}}{k_1}, \quad \text{Sc}_1 = \frac{\nu_1}{D_1} \quad (8)$$

The boundary conditions in dimensionless form are:

- Inlet of the saline solution ($x = 0$)

$$\bar{U} = 1, \quad \bar{V} = 0, \quad \bar{T} = 1, \quad \bar{C} = 1 \quad (9)$$

- Symmetry conditions ($y = 0$)

$$\frac{\partial \bar{U}}{\partial y} = 0, \quad \frac{\partial \bar{T}}{\partial y} = 0, \quad \frac{\partial \bar{C}}{\partial y} = 0, \quad \bar{V} = 0 \quad (10)$$

- Outlet of the saline solution ($x = L$)

$$\frac{\partial \bar{U}}{\partial x} = 0, \quad \frac{\partial \bar{V}}{\partial x} = 0, \quad \frac{\partial \bar{T}}{\partial x} = 0, \quad \frac{\partial \bar{C}}{\partial x} = 0 \quad (11)$$

- Feed saline solution - membrane interface

$$\bar{U} = 0 \quad (12)$$

$$\bar{V} = \frac{J_v}{U_{in1} \rho_1}, \quad \frac{d\bar{T}}{dy} = \frac{l_1(Q_c + Q_L)}{k_1(T_{in2} - T_{in1})}, \quad \frac{d\bar{C}}{dy} = \frac{J_v l_1}{\rho_1 D_{s1} C_{in1}} \quad (13)$$

$Q_L = J_v h_{fg}$ represents the latent heat flux and Q_c is the conduction heat flux.

In the cold domain, the governing equations and their boundary conditions are

$$\frac{\partial \bar{U}}{\partial x} + \frac{\partial \bar{V}}{\partial x} = 0 \quad (14)$$

$$\bar{U} \frac{\partial \bar{U}}{\partial x} + \bar{V} \frac{\partial \bar{U}}{\partial y} = -\frac{\partial \bar{P}}{\partial x} + \frac{1}{\text{Re}_2} \left(\frac{\partial^2 \bar{U}}{\partial x^2} + \frac{\partial^2 \bar{U}}{\partial y^2} \right) \quad (15)$$

$$\bar{U} \frac{\partial \bar{V}}{\partial x} + \bar{V} \frac{\partial \bar{V}}{\partial y} = -\frac{\partial \bar{P}}{\partial x} + \frac{1}{\text{Re}_2} \left(\frac{\partial^2 \bar{V}}{\partial x^2} + \frac{\partial^2 \bar{V}}{\partial y^2} \right) \quad (16)$$

$$\bar{U} \frac{\partial \bar{T}}{\partial x} + \bar{V} \frac{\partial \bar{T}}{\partial y} = \frac{1}{\text{Re}_2 \text{Pr}_2} \left(\frac{\partial^2 \bar{T}}{\partial x^2} + \frac{\partial^2 \bar{T}}{\partial y^2} \right) \quad (17)$$

Where the Reynolds and Prandlt numbers of the cold solution are

$$\text{Re}_2 = \frac{\rho_2 U_{in2} l_2}{\mu_2}, \quad \text{Pr}_2 = \frac{\mu_2 C_{p2}}{k_2} \quad (18)$$

The boundary conditions in dimensionless form are:

- Inlet of the cold solution ($x = L$)

$$\bar{U} = 1, \quad \bar{V} = 0, \quad \bar{T} = 0 \quad (19)$$

- Symmetry conditions

$$\frac{\partial \bar{U}}{\partial y} = 0, \quad \frac{\partial \bar{T}}{\partial y} = 0, \quad \bar{V} = 0 \quad (20)$$

- Outlet of the cold solution ($x = 0$)

$$\frac{\partial \bar{U}}{\partial x} = 0, \quad \frac{\partial \bar{V}}{\partial x} = 0, \quad \frac{\partial \bar{T}}{\partial x} = 0 \quad (21)$$

- The cooling plate's cold side interface

$$\bar{U} = 0 \quad (22)$$

$$\bar{V} = 0 \quad (23)$$

$$\frac{d\bar{T}}{dy} = \frac{l_2(Q_c + Q_L)}{k_2(T_{in2} - T_{in1})} \quad (24)$$

Stephan's law is used to give the general mass flux form Alklaibi and Lior (2005)

$$J_v = K \Delta P_v \quad (25)$$

Where J_v is the vapor flux generated by the membrane, K the permeability of the membrane and ΔP_v the water vapor pressure difference between the membrane sides;

The vapor pressure P_v can be calculated using the Antoine's equation

$$P_v = \exp\left(23.1964 - \frac{3816.44}{T - 46.13}\right) \quad (26)$$

The membrane permeability K is defined for the molecular diffusion as

$$K_M = \frac{\varepsilon D_{v/a} M_v P_T}{\chi \delta_m P_{a,moy} R_u T_{moy,m}} \quad (27)$$

The effect of salt's presence in the solution on the vapor pressure at the hot surface of the membrane side has been considered and the Raoult's Law is used. So that, the vapor pressure at the hot saline solution-membrane interface is expressed as

$$P = (1 - C)P_v \quad (28)$$

Let us consider now the heat transfer mechanism in the AGMD process corresponding to the AGMD configuration (Fig. 1(a)). The total heat is first transferred by convection from the feed solution to the membrane surface where evaporation takes place.

Thus, the total heat involved in such a process can be divided in two parts: the latent heat and the sensible one. The latent one is associated with the evaporation of the liquid water at the hot membrane side. While, the total sensible heat transfer Q_{sens} is transferred from the hot surface of the membrane to the condensation surface by:

- heat conduction across the membranes and the air gap, Q_c ;
- the convective heat transfer associated with the mass transfer of the vapor, Q_v

$$Q_{sens} = Q_c + Q_v = \frac{T_1 - T_2}{R_T} \quad (29)$$

Where T_1 is the temperature at the hot side of the membrane, T_2 is the temperature at the cold side of the cooling plate and R_T is the total heat transfer resistance defined by

$$R_T = R_m + R_g + R_f + R_p \quad (30)$$

R_m , R_g , R_f and R_p are the thermal resistances respectively of the membrane, the humid air gap, the condensate liquid film and of the cooling plate.

$$R_m = \frac{R_{mc} R_v}{R_{mc} + R_v} \quad (31)$$

Where the heat transfer resistance of the solid part of the membrane is

$$R_{mc} = \frac{\delta_m}{k_m} = \frac{\delta_m}{\varepsilon k_a + (1 - \varepsilon) k_{ma}} \quad (32)$$

k_a and k_{ma} are the thermal conductivity of the air, and the membrane material, respectively. The heat transfer resistance of the vapor flow through the membrane pores is

$$R_v = \frac{1}{J_v C_p} \quad (33)$$

The thermal resistance of the air gap is defined as

$$R_g = \frac{R_v R_a}{R_v + R_a} \quad (34)$$

$$R_a = \frac{\delta_g - \delta_f}{k_a} \quad (35)$$

The thermal resistance of the condensate film is defined as

$$R_f = \frac{\delta_f}{k_f} \quad (36)$$

The vapor flux generated by the membrane will condense on the internal side of the cooling plate, and for a thin film, the condensate film thickness δ_f can be calculated as given by (Ramon *et al.* 2009, Bejan 2004).

$$\delta_f(x) = \left(\frac{3\mu_f \int_0^x J_v(x) dx}{g\rho_f(\rho_f - \rho_v)} \right)^{1/3} \quad (37)$$

The thermal resistance of the cooling plate is

$$R_p = \frac{\delta_p}{k_p} \quad (38)$$

Results of this work were expressed in terms of process parameters including the average permeate flux, the conductive heat flux, the total heat transfer and the process thermal efficiency.

The averaged permeate flux is obtained by integrating Eq. (25) over the membrane length L

$$J = \frac{1}{L} \int_0^L J_v(x) dx \quad (39)$$

The averaged conduction heat flux is defined as

$$\overline{Q_C} = \frac{1}{L} \int_0^L Q_C(x) dx \quad (40)$$

The averaged total latent heat flux is

$$\overline{Q_L} = \frac{1}{L} \int_0^L Q_L(x) dx \quad (41)$$

The total heat transfer is

$$\overline{Q_T} = \frac{1}{L} \int_0^L Q_T(x) dx \quad (42)$$

Therefore, the process thermal efficiency can be defined as

$$\eta_t = \frac{\overline{Q_L}}{\overline{Q_T}} \quad (43)$$

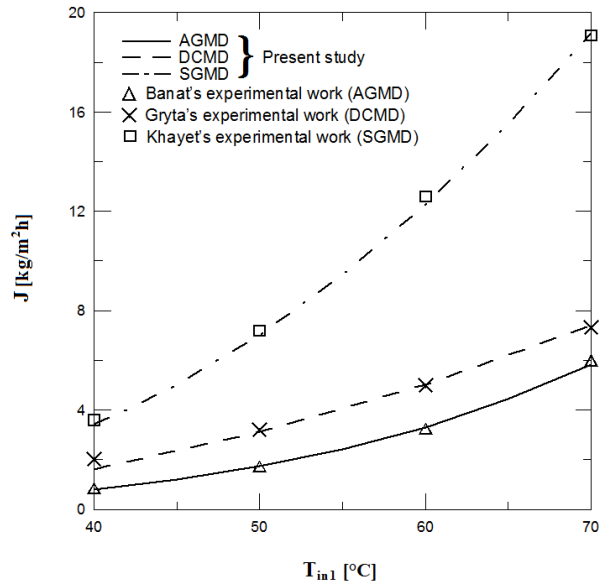


Fig. 2 Inlet temperature's effect on the permeate flux, as in this study, in comparison with the experiments: AGMD (Banat 1994), DCMD (Gryta *et al.* 1997), SGMD (Khayet *et al.* 2000a)

Table 1 Influence of grid size on the permeate flux and the thermal efficiency

| | N_x, N_y | 250,40 | 350,40 | 250,50 | 350,50 |
|------|-----------------------------|---------|---------|---------|---------|
| AGMD | J_v [kg/m ² h] | 5.2920 | 5.2913 | 5.2921 | 5.2914 |
| | η | 0.9242 | 0.9235 | 0.9240 | 0.9237 |
| DCMD | J_v [kg/m ² h] | 17.5420 | 17.5417 | 17.5422 | 17.5418 |
| | η | 0.8634 | 0.8628 | 0.8631 | 0.8629 |
| SGMD | J_v [kg/m ² h] | 3.3641 | 3.3637 | 3.3645 | 3.3639 |
| | η | 0.9293 | 0.9292 | 0.9293 | 0.9291 |

3. Numerical method and validation

The Control Volume Method and the Simpler algorithm (Versteeg and Malalasekera 2007) were used for the numerical solution of the set of governing equations described above.

A grid-dependence analysis of the method of solution was performed as mentioned in Table 1.

The values are practically independent of the chosen grid. We select the grid size of 250, 40 for the simulations conducted in this work.

The computed results for AGMD, DCMD and SGMD were validated by comparison with experimental data (Banat 1994, Gryta *et al.* 1997, Khayet *et al.* 2000a) and were found to be in very good agreement, within about 5%, as shown in Fig. 2.

4. Results and discussion

For all calculations, the following general conditions were considered: $l_1 = l_2 = 2.5$ mm, $L = 25$

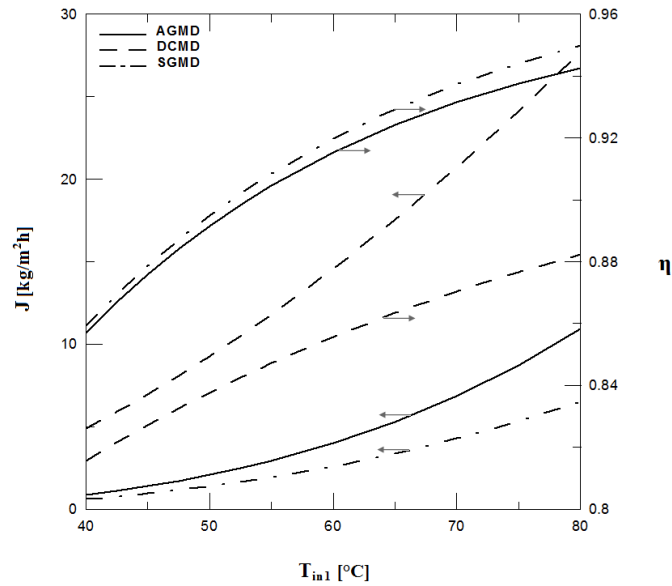


Fig. 3 Effect of inlet temperature of the saline solution on the permeate flux and the thermal efficiency for AGMD, DCMD and SGMD

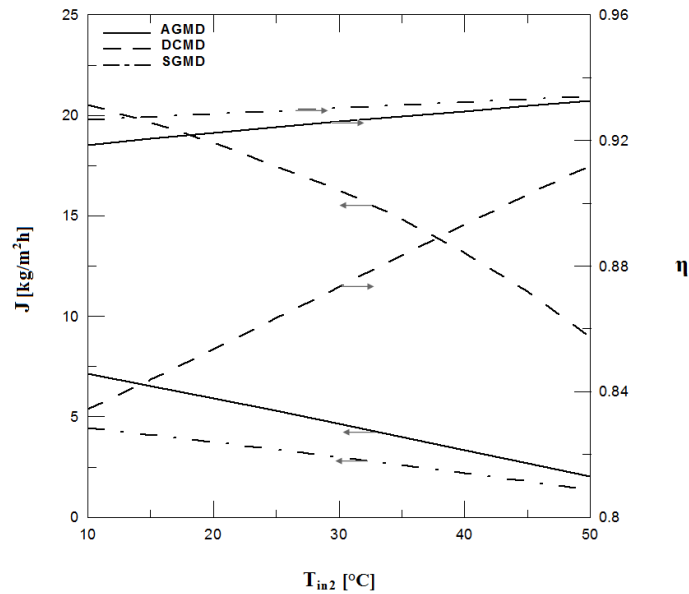


Fig. 4 Effect of the inlet temperature of the cooling solution on the permeate and the thermal efficiency

cm, $U_{in1} = U_{in2} = 0.15$ m/s, $C_{in1} = 0.02$, $T_C = 25^\circ\text{C}$, $\chi = 1.5$, $\varepsilon = 0.8$, $T_{in1} = 65^\circ\text{C}$, $\delta_m = 0.5$ mm, $\delta_g = 2$ mm, $\delta_p = 2$ mm, $K_m = 0.25$ W/mK, $K_p = 50$ W/mK.

Fig. 3 presents the evolution of the permeate flux and the thermal efficiency when varying the inlet temperature of the saline solution for AGMD, DCMD and SGMD. Increasing T_{in1} induces an increase of both parameters J and η .

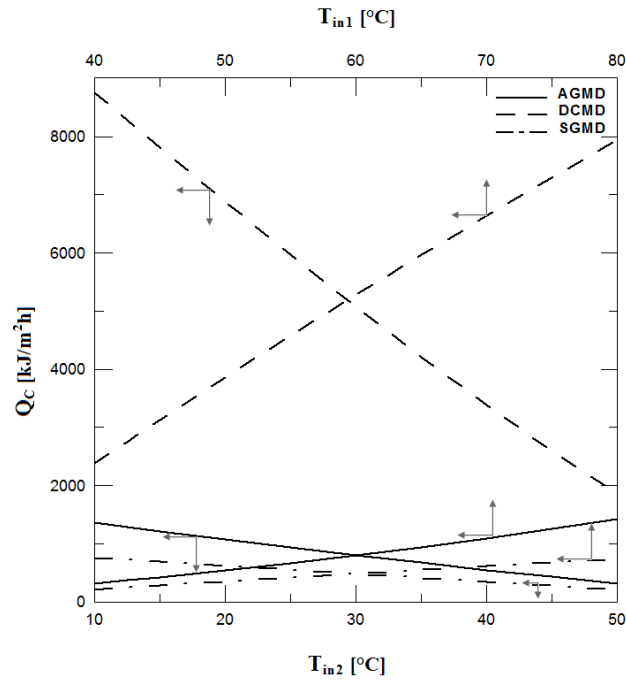


Fig. 5 Effect of the inlet temperatures on the conductive heat transfer

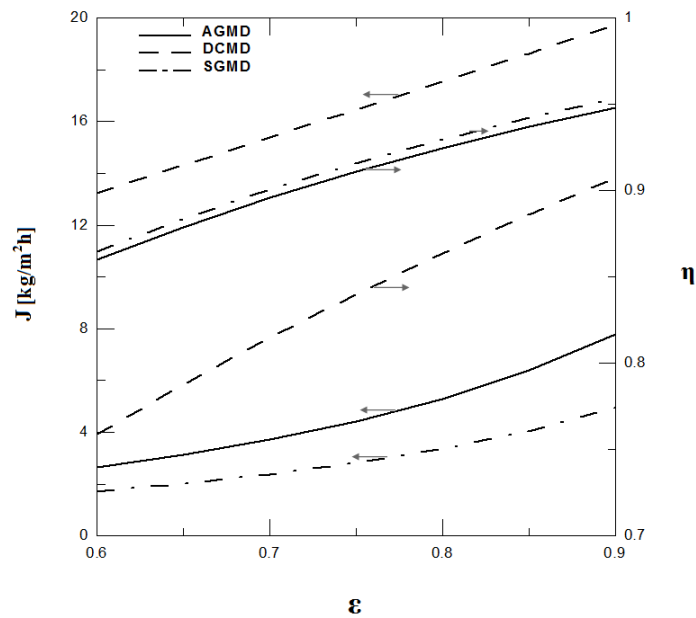


Fig. 6 Effect of membrane porosity on the permeate flux and the thermal efficiency for AGMD, DCMD and SGMD

Under the same operating conditions, it's important to notice that DCMD configuration produces the highest permeate flux in comparison with AGMD and DCMD ones and the lowest

thermal efficiency when increasing T_{in1} from 40 to 80°C. In the other side, SGMD configuration produces the highest thermal efficiency and the lowest permeate flux.

In fact, increasing T_{in1} from 40 to 80°C makes the permeate flux increase by 1140.9%, 466.66%, 985% respectively for AGMD, DCMD and SGMD. In the other side, thermal efficiency increases by 9.92%, 8.22%, 10.47% respectively for AGMD, DCMD and SGMD.

The effect of the temperature of the cooling solution on the three configurations is shown in Fig. 4. Increasing T_{in2} leads to a decrease of J and an increase of η . These variations depend on the configuration adopted. In fact, decreasing T_{in2} from 50 to 10°C makes the permeate flux increase by 254.7%, 129.2%, 228.8% respectively for AGMD, DCMD and SGMD. In the other side, thermal efficiency decreases by 1.5%, 8.55%, 0.85% respectively for AGMD, DCMD and SGMD.

The variation of the conductive heat flux as a function of the inlet temperatures (saline and cooling) is mentioned in Fig. 5. Increasing T_{in1} induces an increase of Q_c while increasing T_{in2} leads to a decrease of the conductive thermal flux.

The variation of the permeate flux and the thermal efficiency as a function of membrane porosity is presented in Fig. 6. In fact, increasing ϵ induces an increase of both J and η for the three MD devices.

Fig. 7 illustrates the effect of the membrane thermal conductivity on the permeate flux and the thermal efficiency. An increase by 113.65, 14.52 and 119.70% for water production respectively for AGMD, DCMD and SGMD devices occurred when k_m increases from 0.05 to 0.35 $\text{Wm}^{-1} \text{K}^{-1}$. The increase of the permeate flux results from the decrease of the effective thermal conductivity of the membrane which leaves much heat for water production.

Fig. 8 shows the effect of the inlet concentration of the saline solution on the permeate flux. One can see that the concentration has a small effect on the water production and the thermal efficiency of the devices. This may present an advantage of MD in comparison with traditional techniques used for desalination.

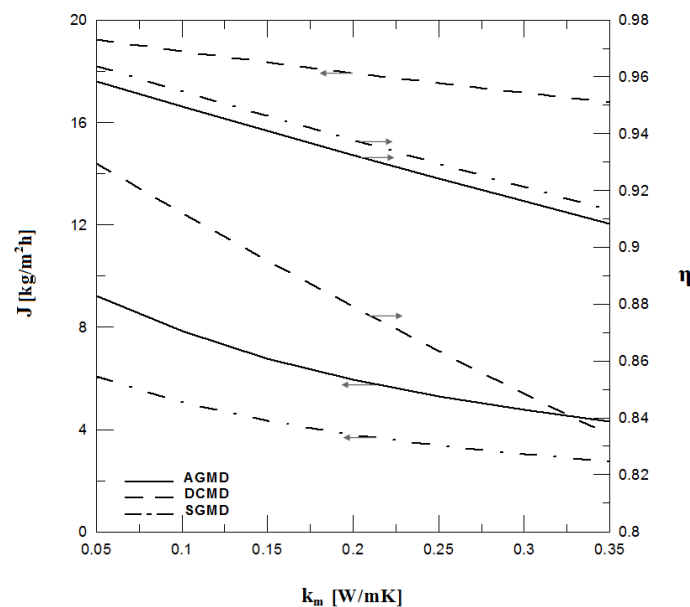


Fig. 7 Effect of membrane thermal conductivity on the permeate flux and the thermal efficiency for AGMD, DCMD and SGMD

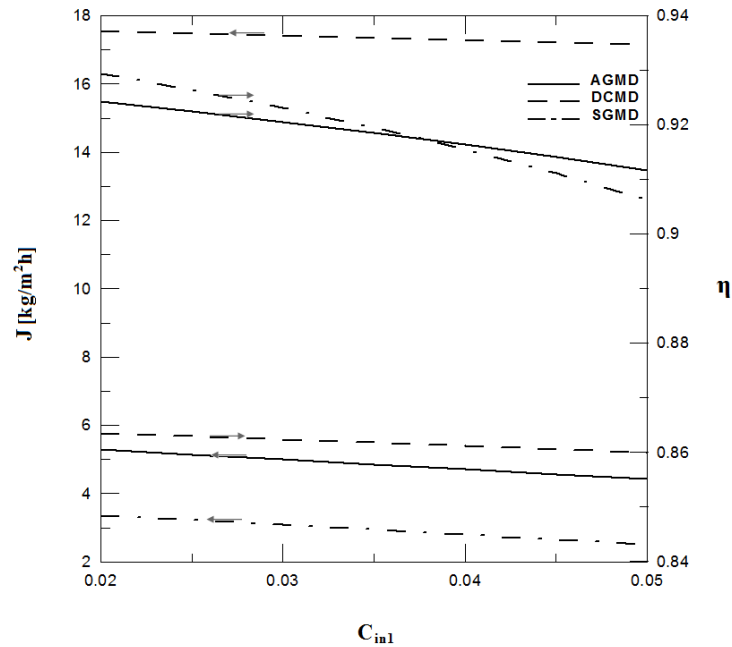


Fig. 8 Effect of inlet concentration on the permeate flux and the thermal efficiency for AGMD, DCMD and SGMD

5. Conclusions

This study presents a comparison between three configurations used in membrane distillation under the same operating conditions. The governing equations expressing the conservation of mass, momentum, energy and species in the hot and cold solutions were developed and solved numerically using the finite volume method. Numerical results were validated with experimental data. The main findings of this study can be summarized in the followings:

- DCMD configuration provides the highest pure water production.
- SGMD configuration shows the highest thermal efficiency.
- For the three configurations, increasing hot inlet temperature or decreasing cold inlet temperature produces higher pure water production.
- For the three configurations, increasing inlet temperatures enhances the thermal efficiency.
- Inlet concentration of the saline solution has no significant effect on process parameters.

Acknowledgments

The second author (Dr. J. Orfi) extends his appreciation to the Deanship of scientific research at King Saud University (Research group Project No: RGP-VPP-091).

References

- Alklaibi, A.M. and Lior, N. (2005), "Transport analysis of air gap membrane distillation", *J. Membr. Sci.*, **255**(1-2), 239-253.
- Amali, A.E., Bouguecha, S. and Maalej, M. (2004), "Experimental study of air gap and direct contact membrane distillation configurations: application to geothermal and seawater desalination", *Desalination*, **168**, 357.
- Bejan, A. (2004), *Convective Heat Transfer*, (3rd Edition), Wiley et Sons, NJ, USA.
- Banat, F. and Simandl, J. (1998), "Desalination by membrane distillation: A parametric study", *Sep. Sci. Technol.*, **33**(1), 201-226.
- Banat, F. (1994), "Membrane distillation for desalination and removal of volatile organic compounds from water", Ph.D. Dissertation; McGill University, Montreal, Canada.
- Banat, F. and Simandl, J. (1994), "Theoretical and experimental study in membrane distillation", *Desalination*, **95**(1), 39-52.
- Chang, H., Tsai, C., Wei, H. and Cheng, L. (2014), "Effect of structure of PVDF membranes on the performance of membrane distillation", *Membr. Water Treat., Int. J.*, **5**(1), 41-56.
- Charfi, K., Khayet, M. and Safi, M.J. (2010), "Numerical simulation and experimental studies on heat and mass transfer using sweeping gas membrane distillation", *Desalination*, **259**(1-3), 84-96.
- Chen, K.K., Xiao, C.F., Huang, Q.L., Liu, H., Liu, H.L., Wu, Y.J. and Liu, Z. (2015), "Study on vacuum membrane distillation (VMD) using FEP hollow fiber membrane", *Desalination*, **375**(2), 24-32.
- Christensen, K., Andresena, R., Tandskov, I., Norddahl, B. and Preez, J.H. (2006), "Using direct contact membrane distillation for whey protein concentration", *Desalination*, **200**(1-3), 523-525.
- Ding, Z., Liu, L., Li, Z., Ma, R. and Yang, Z. (2006), "Experimental study of ammonia removal from water by membrane distillation (MD): The comparison of three configurations", *J. Membr. Sci.*, **286**(1-2), 93-103.
- El-Bourawi, M.S., Ding, Z.M., Ma, R. and Khayat, M. (2006), "Framework for better understanding membrane distillation separation process", *J. Membr. Sci.*, **285**(1-2), 4-29.
- Feng, C., Khulbe, K.C., Matsuura, T., Gopal, R., Kaur, S., Ramakrishna, S. and Khayet, M. (2008), "Production of drinking water from saline water by air-gap membrane distillation using polyvinylidene fluoride nanofiber membrane", *J. Membr. Sci.*, **311**(1-2), 1-6.
- Gábor, R., Steffen, K., Oliver, S., Benjamin, S., Zoltán, K., Gyula, V., Mehrdad, E. and Peter, C. (2015), "Experimental determination of liquid entry pressure (LEP) in vacuum membrane distillation for oily wastewaters" *Membr. Water Treat., Int. J.*, **6**(3), 237-249.
- García-Payo, M.C., Izquierdo-Gil, M.A. and Fernández-Pineda, C. (2000), "Air gap membrane distillation of aqueous alcohol solutions", *J. Membr. Sci.*, **169**(1), 61-80.
- García-Payo, M.C., Rivier, C.A., Marison, I.W. and Von Stockar, U. (2002), "Separation of binary mixtures by thermostatic sweeping gas membrane distillation: II. Experimental results with aqueous formic acid solutions", *J. Membr. Sci.*, **198**(2), 197-210.
- Gryta, M., Tomaszewska, M. and Morawski, A.W. (1997), "Membrane distillation with laminar flow", *Sep. Purif. Technol.*, **11**(2), 93-101.
- Gryta, M., Tomaszewska, M. and Karakulski, K. (2006), "Wastewater treatment by membrane distillation", *Desalination*, **198**(1-3), 67-73.
- Guijt, C.M., Rcz, I.G., Van Heuven, J.W., Reith, T. and De Haan, A.B. (1999), "Modelling of a transmembrane evaporation module for desalination of seawater", *Desalination*, **126**(1-3), 119-125.
- Guijt, C.M., Meindersma, G., Reith, T. and De Haan, A. (2005) "Air gap membrane distillation: 2. Model validation and hollow performance analysis", *Sep. Purif. Technol.*, **43**(3), 245-255.
- Izquierdo-Gil, M.A., García-Payo, M.C. and Fernandez-Pineda, C. (1999), "Air gap membrane distillation of sucrose aqueous solutions", *J. Membr. Sci.*, **155** (2), 291-307.
- Khayet, M., Godino, P. and Mengual, J.I. (2000a), "Nature of flow on sweeping gas membrane distillation", *J. Membr. Sci.*, **170**(2), 243-255.

- Khayet, M., Godino, M.P. and Mengual, J.I. (2000b), "Theory and experiments on sweeping gas membrane distillation", *J. Membr. Sci.*, **165**(2), 261-272.
- Khayet, M., Godino, M.P. and Mengual, J.I. (2003a), "Possibility of nuclear desalination through various membrane distillation configurations: A comparative study", *Int. J. Nucl. Desalination*, **1**(1), 30-46.
- Khayet, M., Godino, M.P. and Mengual, J.I. (2003b), "Theoretical and experimental studies on desalination using the sweeping gas membrane distillation method", *Desalination*, **157**(1-3), 297-305.
- Khayet, M., Godino, M.P. and Mengual, J.I. (2002), "Thermal boundary layers in sweeping gas membrane distillation processes", *Am. Inst. Chem. Eng. J. (AIChE J.)*, **48**(7), 1488-1497.
- Loussif, N. and Orfi, J. (2014), "Effect of slip velocity on air gap membrane distillation process", *Membr. Water Treat., Int. J.*, **5**(1), 57-71.
- Phattaranawik, J., Jiraratananon, R. and Fane, A.G. (2003), "Heat transport and membrane distillation coefficients in direct contact membrane distillation", *J. Membr. Sci.*, **212**(1-2), 177-193.
- Ramon, G., Agnon, Y. and Dosretz, C. (2009), "Heat transfer in vacuum membrane distillation: Effect of velocity slip", *J. Membr. Sci.*, **331**(1-2), 117-125.
- Rommel, M., Koschilowski, J. and Wighaous, M. (2007), *Solar Desalination for the 21st Century*, (Rizzuti et al.), The Netherlands.
- Schofield, R.W., Fane, A.G. and Fell, C.J.D. (1987), "Heat and mass transfer in membrane distillation", *J. Membr. Sci.*, **33**(3), 299-313.
- Sebastian, R.K., Kujawski, W., Bukowska, M., Picard, C. and Larbot, A. (2006), "Application of fluoroalkylsilanes (FAS) grafted ceramic membranes in membrane distillation process of NaCl solutions", *J. Membr. Sci.*, **281**(1-2), 253-259.
- Shirazi, M.M.A., Kargari, A., Tabatabaei, M., Ismail, A.F. and Matsuura, T. (2014), "Concentration of glycerol from dilute glycerol wastewater using sweeping gas membrane distillation", *Chem. Eng. Process.: Process Intensif.*, **78**, 58-66.
- Song, L., Ma, Z., Liao, X., Kosarajua, P.B., Irish, J.R. and Sirkar, K.K. (2008), "Pilot plant studies of novel membranes and devices for direct contact membrane distillation-based desalination", *J. Membr. Sci.*, **323**(2), 257-270.
- Srisurichan, S., Jiraratananon, R. and Fane, A.G. (2006), "Mass transfer mechanisms and transport resistances in direct contact membrane distillation process", *J. Membr. Sci.*, **277**(1-2), 186-194.
- Tomaszewska, M., Gryta, M. and Morawski, A.W. (1995), "Study on the concentration of acids by membrane distillation", *J. Membr. Sci.*, **102**, 113-122.
- Versteeg, H.K. and Malalasekera, W. (2007), *An Introduction to Computational Fluid Dynamics: The Finite Volume Method*, (2nd Edition), Pearson and Prentice Hall, England.
- Wu, C.R., Li, Z.G., Zhang, J.H., Jia, Y., Gao, Q. and Lu, X.L. (2015), "Study on the heat and mass transfer in air-bubbling enhanced vacuum membrane distillation", *Desalination*, **373**, 16-26.

Nomenclature

| | |
|-----------|--|
| C | Mass fraction of NaCl |
| C_p | Specific heat [$\text{Jkg}^{-1}\text{K}^{-1}$] |
| l | half-width of the flow channel [m] |
| D_s | Diffusion coefficient of NaCl [m^2/s] |
| $D_{v/a}$ | Coefficient of vapor-air mass diffusion [m^2/s] |
| g | Acceleration of gravity [m/s^2] |
| h_{fg} | Latent heat of evaporation [J/kg] |
| J_V | length-averaged permeate flux at the hot side of the membrane [$\text{kg}/\text{m}^2\text{h}$] |
| J | local permeate flux at the hot side of membrane, in vapor phase [$\text{kg}/\text{m}^2\text{s}$] |
| K | permeability of the membrane |
| k | Thermal conductivity [W/mK] |
| L | Membrane length [m] |
| M_v | Molar mass of water vapor [kgkmol^{-1}] |
| N_x | Number of nodes along x direction |
| N_y | Number of nodes along y direction |
| P | pressure [Pa] |
| Pr | Prandtl number |
| Q_C | Conductive heat flux [$\text{kJ}/\text{m}^2\text{h}$] |
| Q_L | Latent heat flux [$\text{kJ}/\text{m}^2\text{h}$] |
| Q_T | Total flux [$\text{kJ}/\text{m}^2\text{h}$] |
| R | Universal gas constant [J/kmol K] |
| Re | Reynolds number |
| R_g | Thermal resistance of the air gap |
| R_f | Thermal resistance of the condensate film |
| R_m | Thermal resistance of the membrane |
| R_p | Thermal resistance of the membrane |
| Sc | Schmidt number |
| T | temperature [$^{\circ}\text{C}$] |
| U_{in} | inlet velocity [m/s] |
| U | axial velocity component [m/s] |

| | |
|---------------|--|
| V | radial velocity component [m/s] |
| x | Coordinate along to the solution flow [m] |
| y | coordinate normal to the solution flow [m] |
| μ | Dynamic viscosity [$\text{kgm}^{-1}\text{s}^{-1}$] |
| ν | Cinematic viscosity [m^2s^{-1}] |
| ρ | Density [kgm^{-3}] |
| ε | Porosity |
| χ | Tortuosity |
| δ | Thikness or width [m] |
| η | Process thermal efficiency |

Subscripts

| | |
|-------|---------------------|
| 1 | Hot saline solution |
| 2 | Cooling solution |
| a | air |
| c | cooling plate |
| e | inlet |
| f | condensate film |
| g | air gap |
| in | inlet |
| p | cooling plate |
| m | membrane |
| ma | membrane material |
| moy | Average |
| s | saline solution |
| T | Total |
| v | vapor |